Monte Carlo Simulation of Single- and Binary-Component Adsorption of CO2, N2, and H2 in Zeolite Na-4A

ARTICLE *in* ENERGY & FUELS · JULY 2003

Impact Factor: 2.79 · DOI: 10.1021/ef0300038

3 AUTHORS, INCLUDING:

Ebru Demet Akten
Kadir Has University
14 PUBLICATIONS **341** CITATIONS

Monte Carlo Simulation of Single- and Binary-Component Adsorption of CO_2, N_2, and H_2 in Zeolite Na-4A

E. Demet Akten,[†] Ranjani Siriwardane,[‡] and David S. Sholl*,[†,§]

Department of Chemical Engineering, Carnegie Mellon University, Pittsburgh, Pennsylvania 15213, U.S. Department of Energy, National Energy Technology Laboratory, 3610 Collins Ferry Road, P.O. Box 880, Morgantown, West Virginia 26507-0880, and U.S. Department of Energy, National Energy Technology Laboratory, Pittsburgh, Pennsylvania 15236

Received January 9, 2003. Revised Manuscript Received April 28, 2003

We present a molecular model for the adsorption of CO_2, N_2, H_2, and their mixtures in dehydrated zeolite Na-4A. The interatomic potentials for this model were developed by comparing the results of grand canonical Monte Carlo (GCMC) simulations of single-component adsorption at room temperature with experimental measurements. GCMC simulation is also used to assess the adsorption selectivity of CO_2/N_2 and CO_2/H_2 mixtures, as a function of temperature and gas-phase composition. At room temperature, Na-4A is strongly selective for CO_2 over both N_2 and H_2, although this selectivity decreases slightly as the gas-phase pressure increases. Ideal adsorbed solution theory is shown to give accurate predictions of the adsorption selectivity at low CO_2 partial pressures, provided that a functional form that accurately describes the CO_2 single-component isotherm is used. The adsorption properties of CO_2/N_2 mixtures in Na-4A are compared to the same mixtures in silicalite.

I. Introduction

Zeolites are one possible class of microporous materials that can be used as adsorbents during adsorption-based gas-separation processes, such as pressure swing adsorption (PSA) and temperature swing adsorption (TSA).[1] Several studies have indicated that CO_2 is strongly adsorbed by a variety of zeolites, suggesting that zeolites may play a useful role in CO_2-capture technologies.[2,3] In particular, recent experiments that have examined the competitive adsorption of CO_2 on the zeolite Na-4A from gas mixtures involving N_2 and H_2 showed that this zeolite is strongly CO_2-selective at room temperature.[2]

Although the measurement of single-component adsorption isotherms for zeolites is relatively straightforward experimentally, quantitative measurement of the multicomponent adsorption is considerably more challenging. Molecular modeling methods have been proven to be a useful alternative to examining multicomponent adsorption in zeolites, because if an accurate description of single-component adsorption in a system of interest can be developed, it is relatively easy to extend this description to multicomponent adsorption.[4−7] The use of molecular modeling to generate mixture adsorption data that directly accounts for the atomic-scale factors that influence adsorption in zeolites has been used by several groups to examine the accuracy of approximate descriptions of multicomponent adsorption, such as ideal adsorbed solution theory (IAST).[3,4,8]

In this paper, we develop a molecular model for the adsorption of CO_2, N_2, and H_2 in dehydrated Na-4A by adopting values for the relevant interatomic interaction potentials that yield single-component adsorption isotherms that are in good agreement with our experimental measurements. The details of this model and the simulation techniques that we have applied are presented in Section II. Our experimental methods are described in Section III. The fitting procedure used to determine the interaction potentials is outlined in Section IV. After discussing the single-component adsorption isotherms of CO_2, N_2, and H_2 as a function of temperature in Section V, we turn to the adsorption of binary mixtures of CO_2/N_2 and CO_2/H_2 in Section VI. By performing grand canonical Monte Carlo (GCMC) simulations of these adsorbed mixtures, we are able to assess the accuracy of IAST for these systems directly.

* Author to whom correspondence should be addressed. E-mail: sholl@andrew.cmu.edu.
† Carnegie Mellon University.
‡ National Energy Technology Laboratory−Morgantown.
§ National Energy Technology Laboratory−Pittsburgh.

(1) Yang, R. T. *Gas Separation by Adsorption Processes*; Imperial College Press: London, 1997.
(2) Siriwardane, R. V.; Shen, M.-S.; Fisher, E. P.; Poston, J. A. *Energy Fuels* **2001**, *15*, 279.
(3) Goj, A.; Sholl, D. S.; Akten, E. D.; Kohen, D. *J. Phys. Chem. B* **2002**, *106*, 8367.
(4) Heuchel, M.; Snurr, R. Q.; Buss, E. *Langmuir* **1997**, *13*, 6795.
(5) Lachet, V.; Boutin, A.; Tavitian, B.; Fuchs, A. H. *Langmuir* **1999**, *15*, 8678.
(6) Schuring, D.; Koriabkina, A. O.; de Jong, A. M.; Smit, B.; van Santen, R. A. *J. Phys. Chem. B* **2001**, *105*, 7690.
(7) Yang, J.-H.; Clark, L. A.; Ray, G. J.; Kim, Y. J.; Du, H.; Snurr, R. Q. *J. Phys. Chem. B* **2001**, *105*, 4698.
(8) Challa, S. R.; Sholl, D. S.; Johnson, J. K. *J. Chem. Phys.* **2002**, *116*, 814.

10.1021/ef0300038 CCC: $25.00
Published on Web 05/21/2003

Provided that the single-component isotherms are described with functions that accurately represent the single-component data, IAST predicts the adsorption selectivities with good accuracy for low CO_2 partial pressures. We conclude in Section VII by summarizing our findings and comparing the properties of CO_2/N_2 mixtures in Na-4A with the properties of the same mixture in silicalite, which is another readily available zeolite that shows good CO_2 selectivity.

II. Simulation Model and Methods

A. Crystal Structure of Na-4A. We have simulated gas adsorption in fully dehydrated Na-4A, which has the chemical composition $Na_{12}(AlO_2)_{12}(SiO_2)_{12}$. We assume that the Al atoms are uniformly distributed, so that each framework O atom is bonded to one Si atom and one Al atom. One unit cell of Na-4A consists of eight α cages and eight β cages and has a cubic cell dimension of 24.555 Å,[9] within the *Fm*3*c* space group. The structure of Na-4A was constructed using data supplied by Faux, on the basis of extensive molecular dynamics (MD) simulations of this material.[10,11] The Na^+ cations in this material are called Na(I), Na(II), and Na(III) for cations associated with the six-membered (6R), eight-membered (8R), and four-membered (4R) oxygen rings, respectively. The 64 Na(I) cations in each unit cell lie inside the β cages of the zeolite. MD simulations by Faux and co-workers[10−12] and Shin et al.[13] have shown that Na(I) cations have extremely low mobilities at room temperature. In our simulations, we take advantage of this low mobility by constraining all Na(I) cations to be fixed in position, whereas Na(II) and Na(III) cations are allowed to move. The zeolite framework was assumed to be rigid in all of our calculations.

B. Adsorbate−Adsorbate Interactions. The interactions between pairs of adsorbates of the same species were modeled using well-established interatomic potentials from previous work. The TraPPE force field of Potoff and Siepmann was used for CO_2-CO_2 and N_2-N_2 interactions.[14] This potential quantitatively reproduces the vapor−liquid equilibria of pure CO_2, pure N_2, and their mixtures.[14] H_2-H_2 interactions were described using the interatomic potential of Michels et al.[15] In each of these models, interactions between nonbonded interaction sites are a combination of coulombic interactions between fixed point charges and dispersion interactions represented by 6-12 Lennard-Jones (LJ) potentials. By including point charges at the center of mass of the two diatomic species, the point charges can be chosen to match the known quadrupole moments of the gas-phase molecules. The potential parameters for these three intermolecular potentials are summarized in Table 1. LJ interactions between unlike adsorbates were defined using the Lorentz−Berthelot mixing rules. This combining rule was explicitly used in the development of the TraPPE force field.[14]

Table 1. Summary of Interatomic Potential Parameters Used in This Work[a]

CO_2	N_2	H_2
$\sigma_{O-O} = 3.05$ Å	$\sigma_{N-N} = 3.31$ Å	$\sigma_{H-H} = 2.958$ Å
$\sigma_{C-C} = 2.8$ Å	$\epsilon_{N-N} = 36$ K	$\epsilon_{H-H} = 36.7$ K
$\epsilon_{O-O} = 79$ K	$q_N = -0.482$	$q_H = -0.4829$
$\epsilon_{C-C} = 27$ K	$q_{im} = 0.964$	$q_{im} = 0.9658$
$q_O = -0.35$	$l_{NN} = 1.1$ Å	$l_{HH} = 0.741$ Å
$q_C = 0.70$		
$l_{CC} = 2.32$ Å		
$\sigma_{O-O} = 3.0$ Å	$\sigma_{O-O} = 3.0$ Å	$\sigma_{O-O} = 2.708$ Å
$\sigma_{Na-Na} = 2.85$ Å	$\sigma_{Na-Na} = 2.85$ Å	$\sigma_{Na-Na} = 2.805$ Å
$\epsilon_{O-O} = 22.0$ K	$\epsilon_{O-O} = 87.0$ K	$\epsilon_{O-O} = 72.0$ K
$\epsilon_{Na-Na} = 8.0$ K	$\epsilon_{Na-Na} = 8.0$ K	$\epsilon_{Na-Na} = 8.0$ K

[a] The top set of parameters in each column describes the adsorbate−adsorbate interaction parameters. Charges are in units of e, and q_{im} corresponds to the partial charge located at the middle point of the molecule. The bottom four parameters in each column list the zeolite−zeolite interaction parameters used to define the zeolite−adsorbate interactions via the Lorentz−Berthelot mixing rules.

C. Adsorbate−Zeolite Interactions. The interactions between CO_2, N_2, or H_2 with Na-4A were modeled following the methods of our previous work on CO_2 and N_2 adsorption in silica zeolites.[3] Each interaction center on an adsorbate molecule was allowed to interact with framework oxygen and zeolite cations via both a 6-12 LJ potential and a coulomb potential. For interactions between the adsorbates and the framework Si and Al atoms, only coulombic interactions were included. The partial charges associated with each atomic species were taken from the prior work of Dakrim et al.,[16] namely $q_O = -0.74$ e, $q_{Na} = +0.74$ e, $q_{Al} = 1.42$ e, and $q_{Si} = 0.80$ e. These values are similar to theoretical estimates obtained by the electronegativity equalization formalism.[17,18] The van der Waals interactions represented by the LJ potentials were used to adjust the adsorbate−zeolite interactions to match single-component adsorption data. This procedure is described in detail below. The cutoff distance for adsorbate−zeolite LJ potential is taken as 11.5 Å.

The zeolite framework and Na(I) cations are constrained throughout our calculations; therefore, the potential energy of an adsorbate interacting with these atoms can be calculated efficiently by precomputing this potential on a fine grid and subsequently using an appropriate interpolation scheme.[3,19] We precomputed these portions of the potential energy, using a grid with a resolution of ~0.2 Å and applied cubic spline interpolation to define the potential at an arbitrary point inside this grid.[3] Electrostatic interactions between adsorbates, the mobile cations, and a set of O atoms chosen to maintain charge neutrality in this set of atoms were computed using an Ewald summation.[3]

D. Grand Canonical Monte Carlo Simulations. Single- and binary-component adsorption equilibrium was simulated using GCMC simulations.[20−22] Trial moves for the mobile cations were made by small

(9) Pluth, J. J.; Smith, J. V. *J. Am. Chem. Soc.* **1980**, *102*, 4704.
(10) Faux, D. A.; Smith, W.; Forester, T. R. *J. Phys. Chem. B* **1997**, *101*, 1762.
(11) Faux, D. A. *J. Phys. Chem. B* **1998**, *102*, 10658.
(12) Faux, D. A. *J. Phys. Chem. B* **1999**, *103*, 7803.
(13) Shin, J. M.; No, K. T.; Jhon, M. S. *J. Phys. Chem.* **1988**, *92*, 4533.
(14) Potoff, J. J.; Siepmann, J. I. *AIChE J.* **2001**, *47*, 1676.
(15) Michels, A.; Graaf, W. D.; Seldam, C. A. T. *Physica* **1960**, *26*, 393.
(16) Darkrim, F.; Aoufi, A.; Malbrunot, P.; Levesque, D. *J. Chem. Phys.* **2000**, *112*, 5991.
(17) Mortier, W. J.; Ghosh, S. K.; Shankar, S. *J. Am. Chem. Soc.* **1986**, *108*, 4315.
(18) Uytterhoeven, L.; Dompas, D.; Mortier, W. J. *J. Chem. Soc., Faraday Trans.* **1992**, *88*, 2753.
(19) Makrodimitris, K.; Papadopoulos, G. K.; Theodorou, D. N. *J. Phys. Chem. B* **2001**, *105*, 777.
(20) Soto, J. L.; Myers, A. L. *Mol. Phys.* **1981**, *42*, 971.

displacements of the cations. Trial moves for adsorbed molecules were chosen from adsorbate insertion, adsorbate deletion, rigid body translation, and rigid body rotation.[23] For each Monte Carlo (MC) event, the probability of attempting insertion, removal, translation, and rotation was 30%, 30%, 25%, and 25%, respectively. Chemical potentials were related to gas-phase properties by treating gas phases as being ideal. GCMC simulations typically involved performing 1−5 million MC events to equilibrate the system and then a similar length of simulation during which data was collected.

During GCMC simulations of single-component adsorption, the isosteric heat of adsorption was calculated, using[24]

$$Q_{st} = R\left[T - \left(\frac{\partial E}{\partial N}\right)_T\right] = R\left[T - \left(\frac{\langle N\rangle E - N\langle E\rangle}{\langle N^2\rangle - \langle N\rangle\langle N\rangle}\right)\right]$$

Here, N and E are the number of adsorbed molecules and the contributions to the total potential energy that involve interactions with adsorbed molecules, respectively, and $\langle ...\rangle$ represents a canonical average over all degrees of freedom in the system.

In addition to determining the adsorption isotherms using GCMC simulations, we also directly computed the Henry's law coefficient, K_H, for single-component adsorption using MC integration of the relevant configurational integral.[25] We confirmed that this approach gave results that were in excellent agreement with determinations of K_H made from applying GCMC simulations in the regime of dilute loading.

III. Experimental Methods

To obtain parameters for accurate molecular models for gas adsorption in zeolites, it is crucial to have accurate experimental data for the properties of the systems of interest. Single-component adsorption isotherms, at 25 °C, of pure CO_2, N_2, and H_2 on zeolite Na-4A were obtained up to ~300 psi (~2 × 10^6 Pa), using a volumetric adsorption apparatus. The zeolite sample was obtained from Sud Chemie. Approximately 10 mL of the zeolite were placed in the sample chamber, which was evacuated to ~5 × 10^{-5} Torr at 25 °C prior to each run. The amount of gas adsorbed was calculated using pressure measurements before and after the exposure of the sample chamber to the adsorbing gas. Pressure measurements up to 10^3 Torr were obtained, using an MKS type 660 pressure gauge, and pressures >10^3 Torr were measured using a Setra Datum model 2000 pressure gauge. By measuring the pressure in this manner, it was possible to obtain more-accurate pressure measurements in the low-pressure region (<100 psi) during these experiments than that reported in our previous work.[2]

IV. Adjustment of the Interaction Potential Parameters

The interaction potentials between each adsorbed species and the zeolite atoms were adjusted to yield good agreement with our experimental single-component adsorption data as follows. The partial charges on all atoms were fixed at the values that have been previously discussed, as were the adsorbate−adsorbate interaction parameters. The remaining interaction parameters were specified by defining the LJ interaction potential between pairs of framework O atoms and pairs of Na cations (σ_{O-O}, ϵ_{O-O}, σ_{Na-Na}, ϵ_{Na-Na}), then assuming that the adsorbate−zeolite interactions were given by applying the Lorentz−Berthelot combining rules to the specified potentials. The most important single parameter in this set for determining the overall shape of the adsorption isotherms was found to be σ_{O-O}. The effect on the single-component adsorption isotherm of fixing ϵ_{O-O}, σ_{Na-Na}, and ϵ_{Na-Na} at the values listed in Table 1 for CO_2 and varying σ_{O-O} is illustrated in Figure 1. At low pressures, increasing the value of σ_{O-O} increases the adsorbed amount, because each adsorbate interacts with a larger number of framework O atoms. At high pressures, however, increasing the value of σ_{O-O} decreases the saturation loading, because of the decreased free volume available inside the zeolite. The effects of adjusting the LJ well depths (data not shown) are more straightforward; increasing the well depths leads to stronger adsorption at low pressures but has little effect

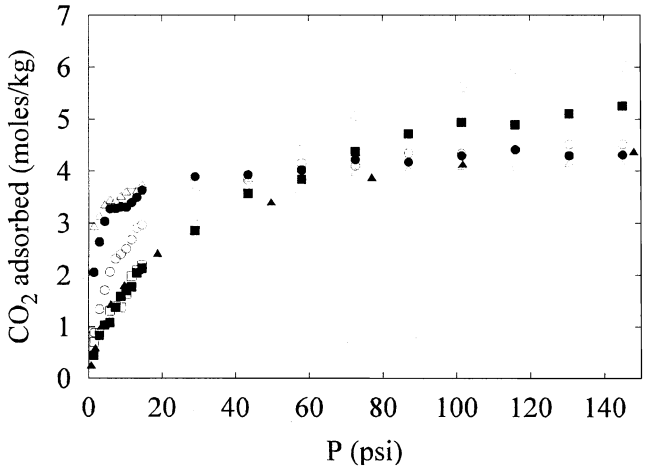

Figure 1. Amount of CO_2 adsorbed at 298 K, as a function of bulk pressure for different values of the LJ parameter, σ_{OO} (σ_{OO} = (□) 2.0, (■) 3.0, (○) 3.5, (●) 4.0, and (△) 4.5 Å; solid triangles denote experimental data).

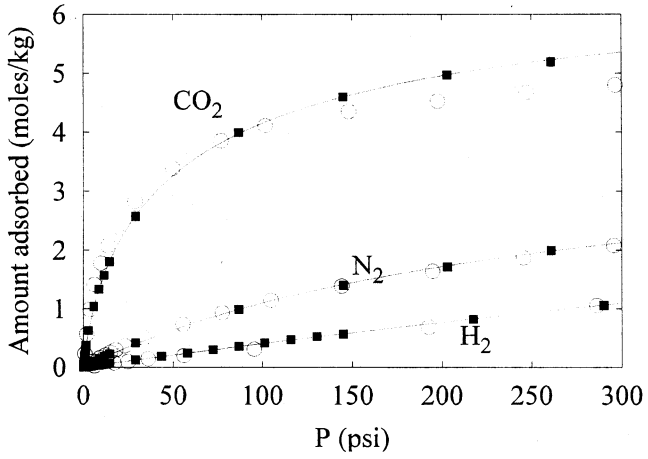

Figure 2. Single-component adsorption isotherms of CO_2, N_2, and H_2 at 298 K obtained from (■) GCMC simulations and (○) experiment. Solid curves are the fitted isotherms described in the text.

(21) Snurr, R. Q.; Bell, A. T.; Theodorou, D. N. *J. Phys. Chem.* **1993**, *97*, 13742.
(22) Karavaias, F.; Myers, A. L. *Langmuir* **1991**, *7*, 3118.
(23) Frenkel, D.; Smit, B. Understanding Molecular Simulation. In *From Algorithms to Applications*; Academic Press: London, 1996.
(24) Vuong, T.; Monson, P. A. *Langmuir* **1996**, *12*, 5425.
(25) June, R. L.; Bell, A. T.; Theodorou, D. N. *J. Phys. Chem.* **1990**, *94*, 1508.

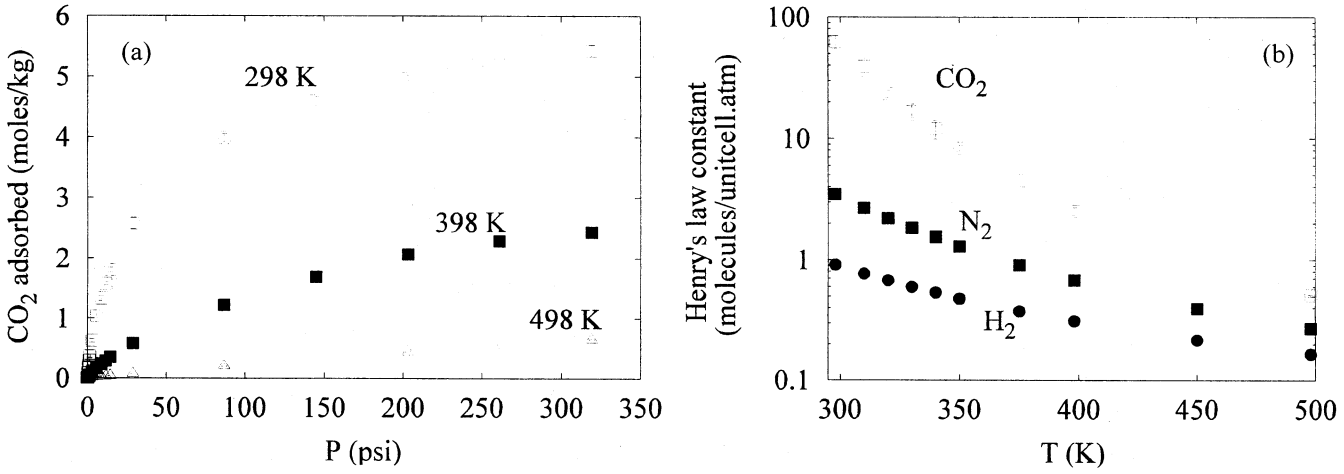

Figure 3. (a) Amount of CO_2 adsorbed at three different temperatures ((□) 298, (■) 398, and (△) 498 K), as a function of pressure. (b) Variation of Henry's law constant, K_h, as a function of temperature for (□) CO_2, (■) N_2, and (●) H_2.

on the saturation loadings. Understanding the general trends resulting from varying each type of potential parameter provided guidance in adjusting the parameters.

To adjust our interaction potentials to fit the experimental data, we first computed the value of K_H. After we determined the parameters that gave K_H values within ~10% of the experimentally observed values, we made minor adjustments to the potential parameters to achieve acceptable agreement between the results from our GCMC calculations and the experimental data over the entire pressure range of our experiments. The resulting potential parameters are summarized in Table 1, and the computed single-component isotherms are compared to the experimental data in Figure 2.

V. Single-Component Adsorption of CO_2, N_2, and H_2

The single-component adsorption isotherms for CO_2, N_2, and H_2 in Na-4A at 298 K predicted by the molecular model previously described are compared with our experimental measurements in Figure 2. We verified that there is no adsorption hysteresis in these systems by separately simulating successive adsorption and desorption of each species along the isotherm. The predicted N_2 and H_2 isotherms are in excellent agreement with the experimental data over the entire range of pressures probed experimentally. CO_2 adsorbs considerably more strongly than the other two gases, and our model slightly overpredicts the experimentally observed saturation loading. This observation is similar to the results observed for an analogous molecular model of CO_2 adsorption in silicalite.[3,19] It is interesting to note that the amount of CO_2 adsorbed on a gravimetric basis in Na-4A at pressures higher than ~50 psi is considerably larger than the amount adsorbed in silicalite under the same conditions, but this amount is similar to that predicted using molecular models of CO_2 adsorption in ITQ-3 and ITQ-7, which are two other all-silica zeolites.[3]

Below, we discuss the prediction of multicomponent adsorption equilibrium from single-component adsorption isotherms using IAST. To accomplish this task, it is necessary to fit appropriate continuous functions to the available single-component adsorption isotherms. The adsorption isotherms predicted by GCMC simulations for N_2 and H_2 are well described by the Langmuir isotherm, $n(P) = ABP/(1 + BP)$. As in our earlier work on CO_2 adsorption in silicalite, we find that this simple isotherm does not describe the observed CO_2 adsorption isotherms in Na-4A. We have fitted the CO_2 isotherms using the isotherm that was determined by Jensen and Seaton:[26]

$$n(P) = K_H P\left\{1 + \left[\frac{K_H P}{\alpha(1 + \kappa P)}\right]^c\right\}^{-1/c}$$

The isotherms determined by fitting these functional forms to our single-component GCMC data at 298 K are shown as solid curves in Figure 2.

The variation in the single-component CO_2 isotherms, as a function of temperature, is shown in Figure 3a. The data in this figure, as with all data in the remainder of this paper, are results that have been calculated from our molecular model. The adsorbed amount, of course, decreases dramatically as the temperature is increased. The amount of CO_2 adsorbed in Na-4A is predicted by our calculations to be very similar to the adsorbed amount in silicalite at 498 K.[3] This observation can be quantified by examining K_H, as a function of temperature, for CO_2 in Na-4A, as shown in Figure 3b. At 498 K, $K_H = 0.037$ mol·kg^{-1}·bar^{-1} in Na-4A, compared to a value of 0.058 mol·kg^{-1}·bar^{-1} in silicalite.[3] The Henry's law coefficients for single-component adsorption of N_2 and H_2 in Na-4A also decrease rapidly as the temperature is increased, as shown in Figure 3b. At 498 K, for N_2, K_H is predicted to have a value of 0.019 and 0.012 mol·kg^{-1}·bar^{-1} in Na-4A and silicalite,[3] respectively. Because the adsorption selectivity for CO_2 over N_2 can be approximated by $K_{H,CO_2}/K_{H,N_2}$(see below), these results suggest that Na-4A exhibits less selectivity than silicalite for CO_2 over N_2 at all temperatures.

The calculated isosteric heat of adsorption for the single-component adsorption of CO_2, N_2, and H_2 in Na-4A at 298 and 498 K are shown in Figure 4. The isosteric heat of adsorption for each species decreases weakly as the temperature increases. Over the limited pressure range examined in Figure 4, Q_{st} is essentially independent of pressure for both N_2 and H_2. This observation

(26) Jensen, C. R. C.; Seaton, N. A. *Langmuir* **1996**, *12*, 2866.

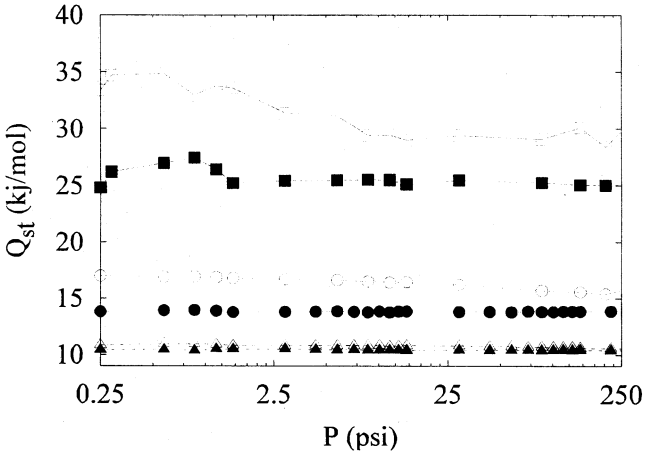

Figure 4. Isosteric heat of adsorption of (□, ■) CO_2, (○, ●) N_2, and (△, ▲) H_2 at 298 K (open symbols) and 498 K (solid symbols).

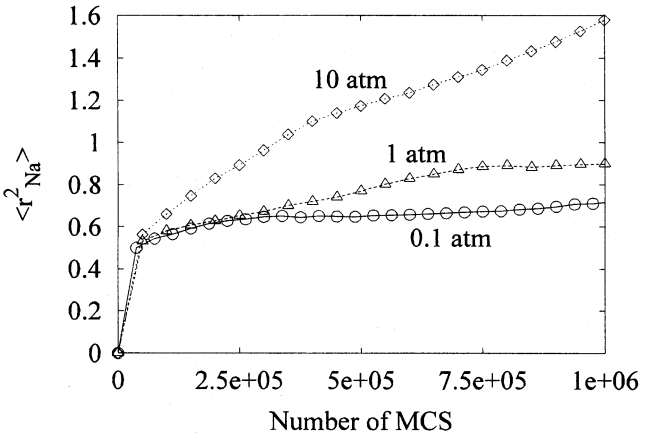

Figure 5. Mean square displacement of Na^+ ions as a function of Monte Carlo steps (MCS) at 498 K and three different CO_2 pressures ((○) 0.1, (△) 1.0, and (◇) 10 atm).

is not surprising, considering that both N_2 and H_2 are well approximated by Henry's law over this pressure range (cf. Figure 2), so the contribution of the adsorbate–adsorbate interactions to Q_{st} is small. The value of Q_{st} for CO_2, in contrast, shows a marked decrease as the density of the adsorbed CO_2 increases. This trend is the opposite of that observed in simulations of silica zeolites; in these materials, the value of Q_{st} is found to increase as the adsorbate density increases.[3] The observed trend for Na-4A indicates that the first few CO_2 molecules that adsorb in each unit cell occupy binding sites with slightly stronger binding energies than those available to subsequent adsorbed molecules. Pressure is shown on a logarithmic scale in Figure 4, to highlight the dependence of Q_{st} over the range of pressures that corresponds to the low- and moderate-loading regimes of CO_2 adsorption at 298 K.

Although MC simulations cannot give quantitative information on the dynamics of atoms within the simulation system, they can be used to gain qualitative insight into this issue. Figure 5 shows the mean squared displacements of the mobile Na(II) and Na(III) cations in our GCMC simulations, in terms of MC events for GCMC simulations of CO_2 adsorption at 498 K. In all three examples shown in Figure 5, the net motion of these cations during the simulation is very slight and is most accurately described as consisting of short-range vibrations about each cation's mean position. This observation is qualitatively consistent with the more detailed MD studies of cation mobility in Na-4A by Faux and co-workers[10–12] and Shin et al.[13]

VI. Binary Adsorption in Na-4A

One important use of molecular models for adsorption in microporous materials is to examine multicomponent adsorption. Multicomponent adsorption is of obvious importance for practical applications but is inconvenient to measure experimentally. We have performed GCMC calculations with the previously described molecular model to examine the adsorption of CO_2/N_2 and CO_2/H_2 mixtures in Na-4A.

In our initial calculations, we fixed the gas-phase composition and varied the total pressure to examine the mixture isotherms. For each system shown below, the gas-phase composition was chosen to generate an equimolar adsorbed mixture in the low-pressure limit. In this limit, IAST is valid, and the selectivity of the adsorbent for species 1 over species 2 is given simply by $K_{H,1}/K_{H,2}$, where $K_{H,i}$ are the single-component Henry's law constants.[1,8] The selectivity resulting from our predicted single-component Henry's law constants and the gas-phase compositions used in our GCMC calculations of CO_2/N_2 and CO_2/H_2 mixtures are summarized in Table 2. The mixture isotherms determined from our GCMC calculations for CO_2/N_2 and CO_2/H_2 mixtures under these conditions are shown in Figure 6. As for the single-component isotherms presented previously, no hysteresis was observed in these calculations. If the adsorption selectivity for these mixtures was independent of pressure, equimolar adsorbed mixtures would be observed at all pressures in our calculations. This simple description is reasonably accurate for the CO_2/N_2 mixtures (see Figure 6a), although slight deviations from the equimolar state are observed at 298 K. Stronger deviations are observed at 298 K for the CO_2/H_2 mixture (see Figure 6b).

The variation in the adsorption selectivity for CO_2/N_2 and CO_2/H_2 mixtures at 298 K is shown in Figure 7. In this figure, the data points are the same GCMC results shown in Figure 6. The solid curves in Figure 7 represent the selectivities predicted by applying IAST to the single-component isotherms described previously. IAST is quantitatively accurate in predicting the 35% decrease in selectivity that occurs for this CO_2/H_2 mixture as the pressure is increased from low pressures to 700 psi (see Figure 7b). The discrepancies that occur between the GCMC data and IAST predictions for total pressures between ~10 and 100 psi mainly stem from the difficulty in sampling the adsorbed amounts in GCMC calculations with very low total loadings accurately. In this pressure range, the number of adsorbed molecules per unit cell is considerably less than 1, and small fluctuations in the adsorbed amount of either species become greatly amplified in the observed selectivity. In principle, this difficulty could be alleviated using larger simulation volumes in this regime. Although the selectivity of CO_2/N_2 adsorption varies less with pressure than for CO_2/H_2 mixtures, IAST is somewhat less accurate in predicting the selectivity of CO_2/N_2 mixtures under the conditions shown in Figure 7. IAST underpredicts the CO_2/N_2 selectivity by ~10% for pressures higher than ~50 psi.

Table 2. Values of the Adsorption Selectivity of CO_2 over N_2 and CO_2 over H_2 at 298, 398, and 498 K in Na-4A in the Low-Pressure Limit and the Corresponding Mixture Compositions That Were Used in the GCMC Simulation of Binary Adsorption

	$T = 298$ K		$T = 398$ K		$T = 498$ K	
	composition	selectivity	composition	selectivity	composition	selectivity
CO_2/N_2	94.9% N_2, 5.1% CO_2	18.75	78.8% N_2, 21.2% CO_2	3.71	65.2% N_2, 34.8% CO_2	2.87
CO_2/H_2	98.6% H_2, 1.4% CO_2	70.65	89.0% H_2, 11.0% CO_2	8.08	75.5% H_2, 24.5% CO_2	3.07

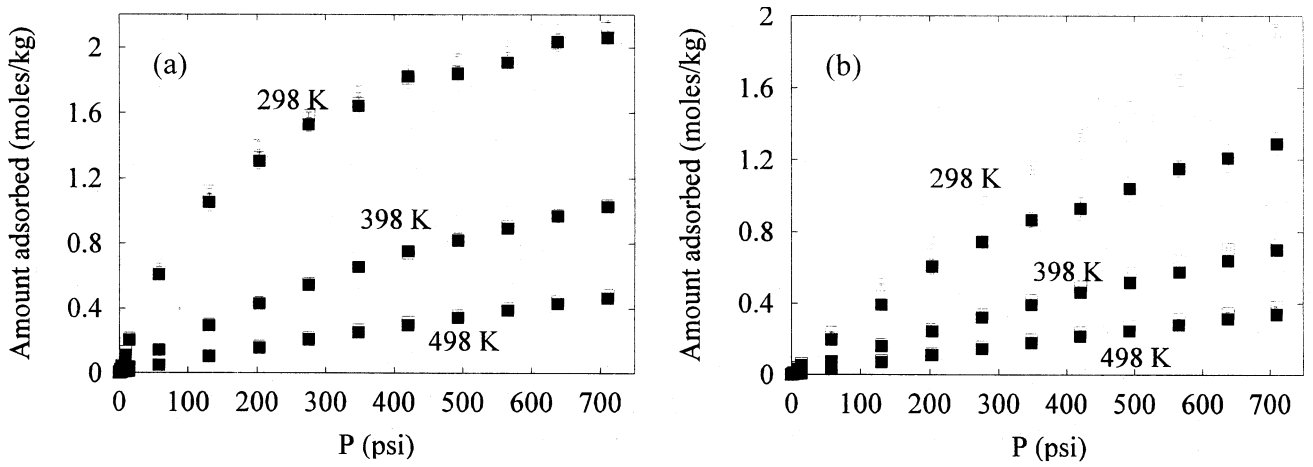

Figure 6. Adsorption isotherms of each component in the two-component mixture of (a) CO_2/N_2 and (b) CO_2/H_2, at 298, 398, and 498 K. (CO_2 is represented by filled symbols in both figures while the open symbols correspond to N_2 and H_2.)

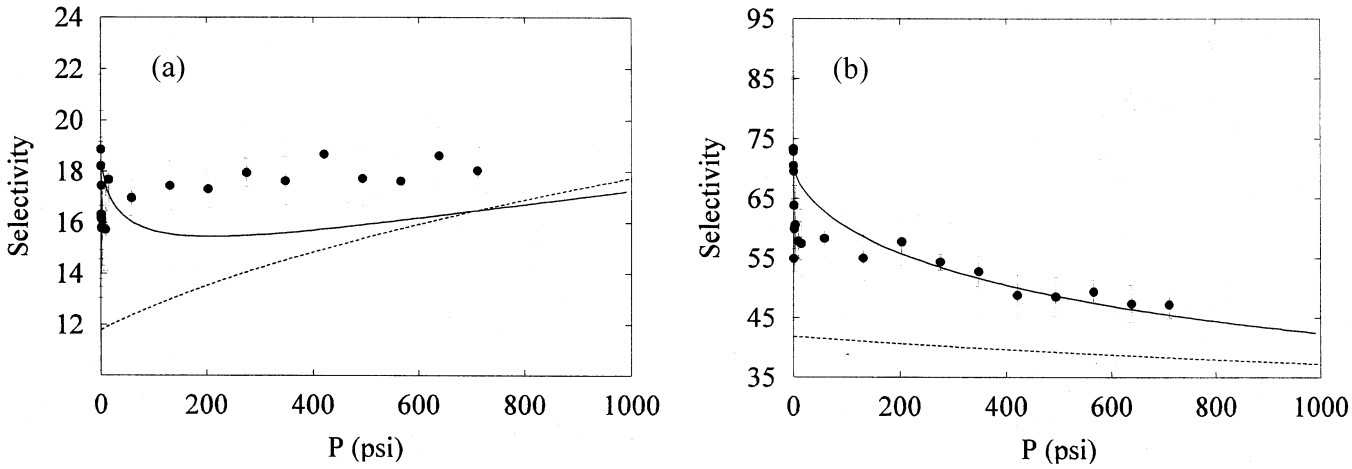

Figure 7. Selectivity of (a) CO_2 over N_2 and (b) CO_2 over H_2, as a function of the total bulk pressure obtained from GCMC (data points) compared to the estimate by IAST (shown with solid line). The dashed line in both figures represents the IAST estimate when using the Langmuir equation instead of the Jensen−Seaton equation for fitting the single-component isotherm of CO_2.

The general trends in the selectivities shown in Figure 7 are similar to those observed in earlier simulation of xenon/argon and xenon/CH_4 mixture adsorption in Na-4A by van Tassel et al.[27] At dilute concentrations, the adsorbed amounts are dominated by the adsorption strength of the individual species. When one species is significantly smaller than the other, as is the case for H_2 compared to CO_2 in our work and argon compared to xenon in the work of van Tassel et al.,[27] the adsorption selectivity shifts toward the smaller species at sufficiently high bulk pressures. This effect is greatly reduced for species with similar sizes, such as N_2/CO_2 in our calculations and xenon/CH_4 in the work of van Tassel et al.[27] These general trends can also be understood by applying IAST to single-component isotherms that are taken to have the Langmuir form and systematically varying the relative Henry's constants and saturation loadings of the two adsorbed species.[8]

The importance of using accurate single-component isotherms when applying IAST is also illustrated in Figure 7. In Figure 7a and b, the lower curve is the prediction that is made with IAST when the single-component isotherm data for CO_2 is fitted with a Langmuir isotherm rather than the Jensen−Seaton isotherm. In making this comparison, we have followed the standard procedure of fitting the Langmuir isotherm to the entire isotherm. The Langmuir isotherm does not accurately describe the full shape of the observed CO_2 isotherm; therefore, this fitting procedure results in a somewhat inaccurate estimate of K_H for CO_2. For this reason, the selectivity predicted by IAST from the Langmuir isotherms does not match the true selectivity

(27) Van Tassel, P. R.; Davis, H. T.; McCormick, A. V. *Langmuir* **1994**, *10*, 1257.

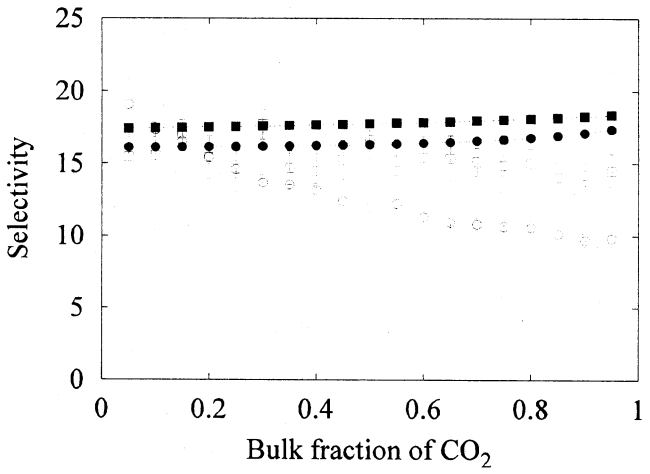

Figure 8. Selectivity of CO_2 over N_2 as a function of the bulk fraction of CO_2 in the mixture obtained from GCMC (open symbols), compared to the estimate by IAST (filled symbols) at two different bulk pressures ((□, ■) $P = 0.1$ atm and (○, ●) $P = 1$ atm).

in the limit of low pressures. Even ignoring this difficulty, neither of the resulting IAST predictions does a particularly good job of describing the variation in the adsorption selectivity with pressure.

The binary adsorption results previously examined only adsorbed mixtures with approximately equimolar compositions. It is, of course, interesting to examine how accurately IAST can predict the adsorption selectivities of these mixtures under other conditions. In Figure 8, the adsorption selectivity of CO_2 over N_2 is shown as a function of the gas-phase composition at two gas pressures: 0.1 and 1.0 atm at 298 K. The data in Figure 7 correspond to the lowest gas-phase composition of CO_2 shown in Figure 8. IAST predicts that the adsorption selectivity is essentially independent of the gas-phase composition for these conditions (filled symbols in Figure 8). Our GCMC results indicate that the actual selectivity decreases markedly as the gas-phase mole fraction of CO_2 increases. When the gas pressure is 1.0 atm, IAST overpredicts the adsorption selectivity by as much as 70% for Na-4A in equilibrium with a CO_2-rich gas phase. These results suggest that, although IAST can quantitatively predict the adsorption selectivities of CO_2 over N_2 and H_2 in Na-4A at room temperature when the partial pressures of CO_2 are small, quantitative prediction of these selectivities is not possible using IAST for moderate or high CO_2 partial pressures.

VII. Conclusion

We have presented a molecular model for the adsorption of CO_2, N_2, H_2, and their mixtures in a dehydrated zeolite, Na-4A. The interatomic potentials for this model were adjusted to reproduce our experimental measurements of single-component gas adsorption at 298 K. As we have observed previously for silica zeolites, the single-component adsorption isotherm for CO_2 at room temperature in Na-4A cannot be fitted accurately using a Langmuir isotherm. This isotherm can be accurately described using a functional form proposed by Jensen and Seaton.[26] Using this fitted isotherm for CO_2 and Langmuir isotherm fits of our single-component N_2 and H_2 data, ideal adsorbed solution theory (IAST) can be used with almost-quantitative accuracy to predict the adsorption selectivities that are observed in our GCMC simulations on binary-mixture adsorption. This accuracy does not extend, however, to adsorbed mixtures in equilibrium with gas phases that have moderate or high CO_2 partial pressures. In these cases, IAST seems to overestimate the actual adsorption selectivity substantially.

It is interesting to compare the adsorption of CO_2/N_2 mixtures in Na-4A with the properties of the same mixtures in silicalite. We have previously presented data for CO_2/N_2 adsorption in silicalite using the same type of molecular model that has been presented here for Na-4A.[3] The gravimetric saturation loading of CO_2 is much greater in Na-4A than in silicalite, but the selectivity for CO_2 over N_2 is better in silicalite than in Na-4A over a broad range of conditions. In the limit of low pressures, where the adsorption selectivity is determined by the ratio of the single-component Henry's constants, the selectivity of silicalite for CO_2 over N_2 decreases from 27 at room temperature to 4.6 at 498 K, whereas the selectivity for Na-4A decreases from 18.8 to 2.9 over the same range. Perhaps more importantly, the adsorption selectivity at room temperature in silicalite increases as the bulk gas pressure increases. In Na-4A, we observed the opposite trend under all the conditions that we have examined: namely, increasing the bulk gas pressure causes the adsorption selectivity to decrease.

Acknowledgment. D.S.S. is an Alfred P. Sloan Fellow and a Camille Dreyfus Teacher−Scholar. Helpful discussions with Professor Daniela Kohen are gratefully acknowledged.

EF0300038